Proceedings of the 3rd ITB Graduate School Conference ISSN: 2963-718X
Enhancing Creativity in Research Through Developing Innovative Capabilities
December 21, 2022

Open-system Magmatic Process at Agung Volcano, Bali, Indonesia: Evidence from Phenocryst Compositions and Textures

Adzkia Noerma Arifa[1, *], I Gusti Bagus Eddy Sucipta[2], & Idham Andri Kurniawan[2]

[1]Geological Engineering Master Program, Faculty of Earth Sciences and Technology, Institut Teknologi Bandung
[2]Petrology, Volcanology and Geochemistry Research Group, Geological Engineering, Faculty of Earth Sciences and Technology, Institut Teknologi Bandung
*Email: adzkiaarifa@gmail.com

Abstract. Agung volcano is an active stratovolcano located in Bali, Indonesia. It is the highest volcano on Bali at 3142 m a.s.l. Samples are collected along the flanks and represent each lava unit. In term of petrology, samples are porphyritic high alumina basalt, basaltic andesite and andesite with inhomogeneous phenocrysts of plagioclase, clinopyroxene, orthopyroxene, olivine, amphibole and titano-magnetite. Plagioclase phenocrysts frequently show fine sieve, resorption surface, coarse sieve and oscillatory zoning texture. Augite and enstatite phenocrysts display texture less zone and monotonous crystal zoning. Olivine phenocrysts are less abundant and present reaction rims of Mg-rich of orthopyroxene and titano-magnetite or Ca-poor clinopyroxene. Hornblende micro-phenocrysts just found in AD 1963 andesitic lava. They have reaction rims composed of augite, feldspar and symplectitic intergrowth of titanomagnetite. Plagioclase, pyroxene and olivine phenocrysts frequently display increases in Mg or Ca contents within mid-crystals. Dissolution, resorption and reverse zoning suggest open system magmatic behavior of repeated mafic magma recharge and also mineral-magma disequilibrium.

Keywords: *Agung volcano; disequilibrium; magma recharge; open system.*

1 Introduction

Indonesia is one of the most densely inhabited nations and home to hundreds of volcanoes. Most volcanoes belong to the Sunda volcanic arc, stretching from Sumatera to Banda Island as the result of subducted the Indo-Australia plate beneath the Eurasia plate. One of the active volcanoes is the Agung volcano on Bali Island. It had recorded effusive and explosive eruptions with the average eruptive frequency of one VEI >= 2-3 eruptions per century [1]. The biggest eruption was in 1963, following 120 years of dormancy, which caused a thousand fatalities [2]. Here we employ petrological and geochemical studies on lavas from the AD 1963 eruption to before the AD 1040 eruption of the Agung volcano

(Table 1). The data is used to understand the magmatic process beneath the Agung volcano as the minerals respond texturally and compositionally to changing magmatic environments.

Table 1 Lava units of Agung volcano [3] and the samples position.

Age	Stratigraphic Unit			Eruption Activity	Lava Flow	Sample Position
Relative	Absolute	Khuluk	Gumuk			
Quarternary	AD 1963	Agung	Pawon	Flank	AI 14	BEL-1 & BEL-4
					AI 13	
	AD 1830 ± 40				AI 12	GA-TU 1
					AI 11	MTG-3
					AI 10	GA-180805 MT
	AD 1040 ± 40				AI 9	GA-DA 1
					AI 8	
					PI	BPW-2
					AI 7	DTH-1
					AI 6	
					AI 5	
					AI 4	GA-TD 1
					AI 3	
					AI 2	
					AI 1	

2 Geological Setting

The Agung volcano situated at latitude 08°20’20” S and longitude 115°30’30” E dominated the eastern part of Bali (Figure 1). It is one of the volcanoes in the western area of the Lesser Sunda in the central part of the Sunda volcanic arc. The oceanic crust that subducts beneath Agung volcano is some of the oldest in the Indian Ocean. It lies approximately 300 km north of the Java Trench and is situated about 162 km above the Benioff Zone [4].

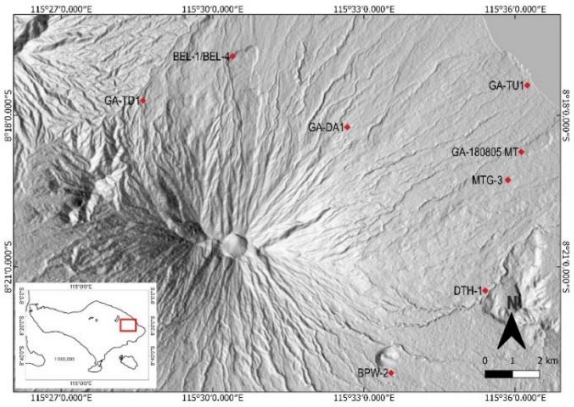

Figure 1 Sampling points map overlain onto a DEM. The inset map shows the location of Agung volcano (red) on the Bali Island.

Based on the geochemistry data, the affinity magma of Agung volcano is calc-alkaline series which are typical of those many Sunda volcanic arc. Based on discriminant diagrams (immobile trace element; La, Ce, Sm, Nb, Th, Y, Zr, Yb) for intermediate volcanic rocks, the tectonic environment of the Agung volcano is an island arc (Figure 2). The Quaternary eruptions of the Agung volcano generated basaltic to andesitic lava in composition and pyroclastic fall or flow deposits around the flanks.

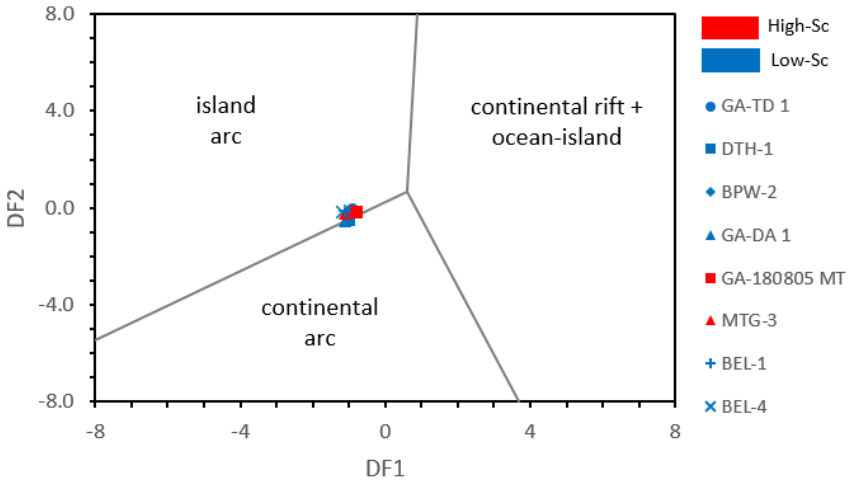

Figure 2 Discriminant diagram [5] to identify tectonic environment.

3 Methodology

Lava samples were prepared for petrology and mineralogy analyses. The optical microscope was used to obtain important information on mineral texture, abundance, and distribution. Polished sections, which were carbon coated, were used to examine mineral chemistry. The analytical instrument used to obtain mineral chemical composition was scanning electron microscope-energy dispersive X-ray spectroscopy (SEM-EDS) JEOL JSM-IT-300. We used back-scattered electron images to identify the compositional changes. Point and line analyses on olivine, pyroxene, plagioclase and titanomagnetite were acquired using 15kV accelerating voltage in high vacuum mode and ZAF correction procedure.

The samples were cut to remove the weathered surface before whole-rock composition analysis. Major element compositions of whole-rock were analyzed using an X-ray fluorescence spectrometer (XRF) and trace element compositions of whole rock were analyzed using ICP-MS/OES. Eight samples have LOI values <0.01 wt.% and one sample has LOI of 0.28 wt.% (Table 2).

Table 2 Major and trace elements data for lava of Agung volcano.

Sample	GA-TD 1	DTH-1	BPW-2	GA-DA 1	GA-180805 MT	MTG-3	GA-TU 1	BEL-1	BEL-4
Lava Unit [3]	Al4	Al7	Pl	Al9	Al10	Al11	Al12	Al14	Al14
Major elements (wt.%) recalculate dry									
SiO_2	57.69	54.59	54.43	60.09	53.59	52.41	51.43	58.53	57.61
TiO_2	0.80	0.85	0.86	0.68	0.97	1.03	1.20	0.73	0.79
Al_2O_3	17.40	20.58	20.76	17.35	18.13	19.64	17.78	17.39	17.27
Fe_2O_3t	8.31	7.75	7.61	7.31	10.11	9.67	11.57	7.68	8.22
MnO	0.19	0.17	0.17	0.18	0.19	0.19	0.21	0.17	0.18
MgO	3.29	2.47	2.52	2.31	4.25	3.72	4.98	3.17	3.50
CaO	6.99	8.71	8.76	6.63	8.26	8.88	8.56	7.12	7.35
Na_2O	3.43	3.32	3.44	3.33	2.99	3.14	2.92	3.25	3.21
K_2O	1.60	1.29	1.18	1.86	1.24	1.09	1.11	1.71	1.61
P_2O_5	0.29	0.27	0.27	0.28	0.27	0.23	0.24	0.26	0.27
LOI (wt.%)	*<0.01*	0.28	*<0.01*	*<0.01*	*<0.01*	*<0.01*	*<0.01*	*<0.01*	*<0.01*
Trace elements (ppm)									
La	15.00	12.30	12.40	20.00	11.20	10.50	11.30	15.70	15.50
Ce	31.60	26.80	26.20	42.50	24.80	22.60	24.80	34.30	34.00
Sm	4.50	3.60	4.10	5.10	3.70	3.70	4.20	4.30	4.70
Nb	5.10	3.30	3.70	4.60	3.80	3.30	2.90	5.10	4.90
Th	3.57	2.29	2.69	4.51	2.31	1.98	1.89	4.06	3.98
Y	23.60	21.90	21.50	28.10	20.70	21.30	22.30	23.10	24.10
Zr	118.00	89.50	87.90	163.00	85.90	80.10	83.40	126.00	125.00
Yb	2.90	2.30	2.50	3.10	2.30	2.50	2.70	2.90	3.10

4 Result

The lavas of Agung and its flank eruption fall into three main groups; (1) high alumina basalts, (2) medium-K basaltic andesite, (3) medium-K andesite. They are distinguished based on SiO_2, Na_2O and K_2O variation diagrams. In addition, two magma types are identified based on scandium (Sc) content, i.e. high-Sc (>20 ppm) and low-Sc (≤20 ppm) (Figure 3).

High alumina basalt (Figure 4). The high-Al basalt is inferred to be A12 lava unit. It dated to AD 1843+-40 [3]. This lava is designated based on SiO_2 content of 51.43 wt.%, more than 17 wt.% of Al_2O_3 and high-Sc (>20 ppm). It has porphyritic texture consisting of olivine (Fo65-76), plagioclase (An38-86), a small amount of augite (Mg#67-81) and enstatite (Mg#67-72). Olivine phenocrysts have zoning and frequently with thick reaction rims of pigeonite. Plagioclase phenocrysts are normal zoning from core to rim-crystal but compositional inversion in mid-crystal. Moreover, they dominantly display fine sieve texture, coarse sieve texture and glomerocrysts. The characteristic of Al-enrichment is due to the more prolonged episode of clinopyroxene or olivine crystallization before the appearance of plagioclase [6].

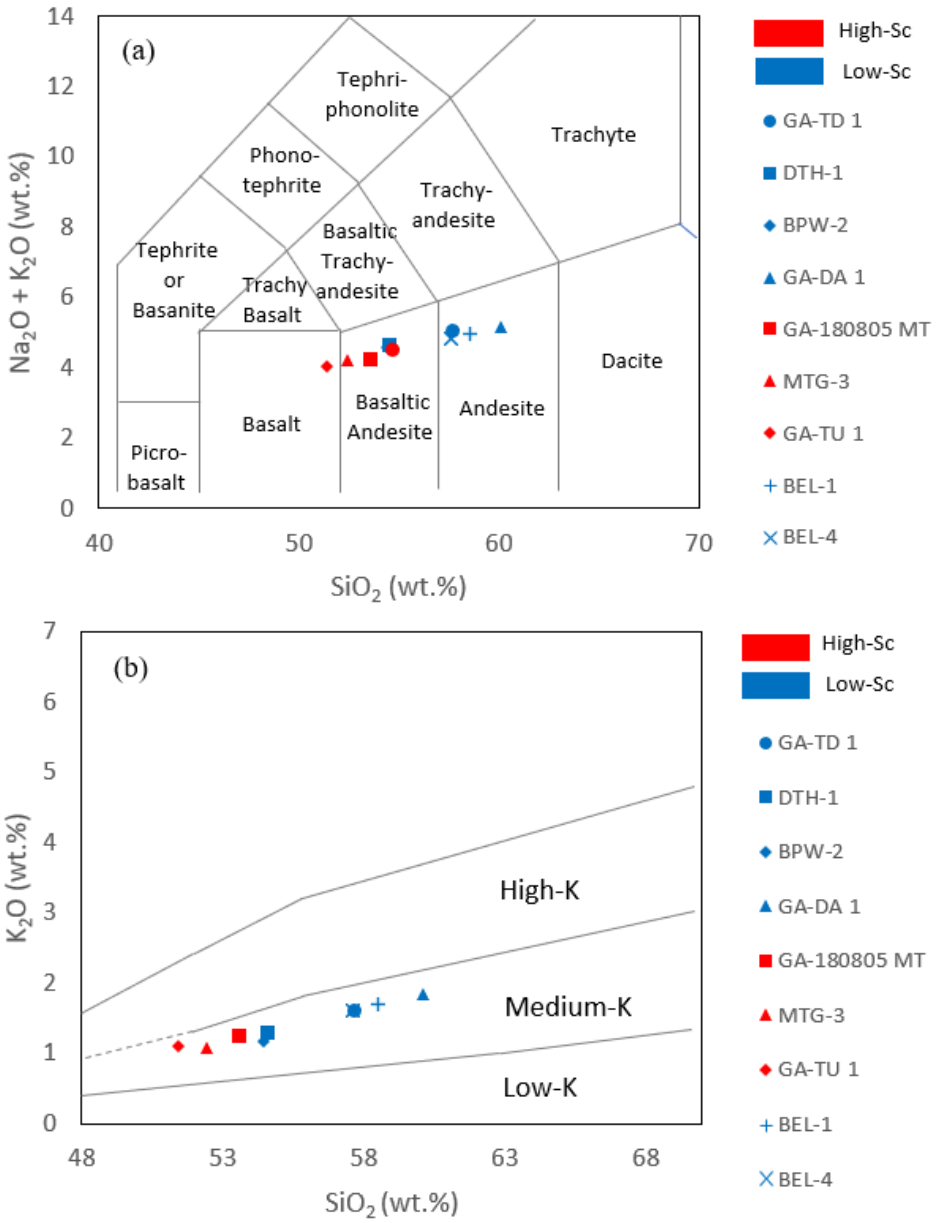

Figure 3 **(a)** Total alkali (TAS) [7] and **(b)** K_2O versus silica [8] classification diagram for lava of Agung volcano.

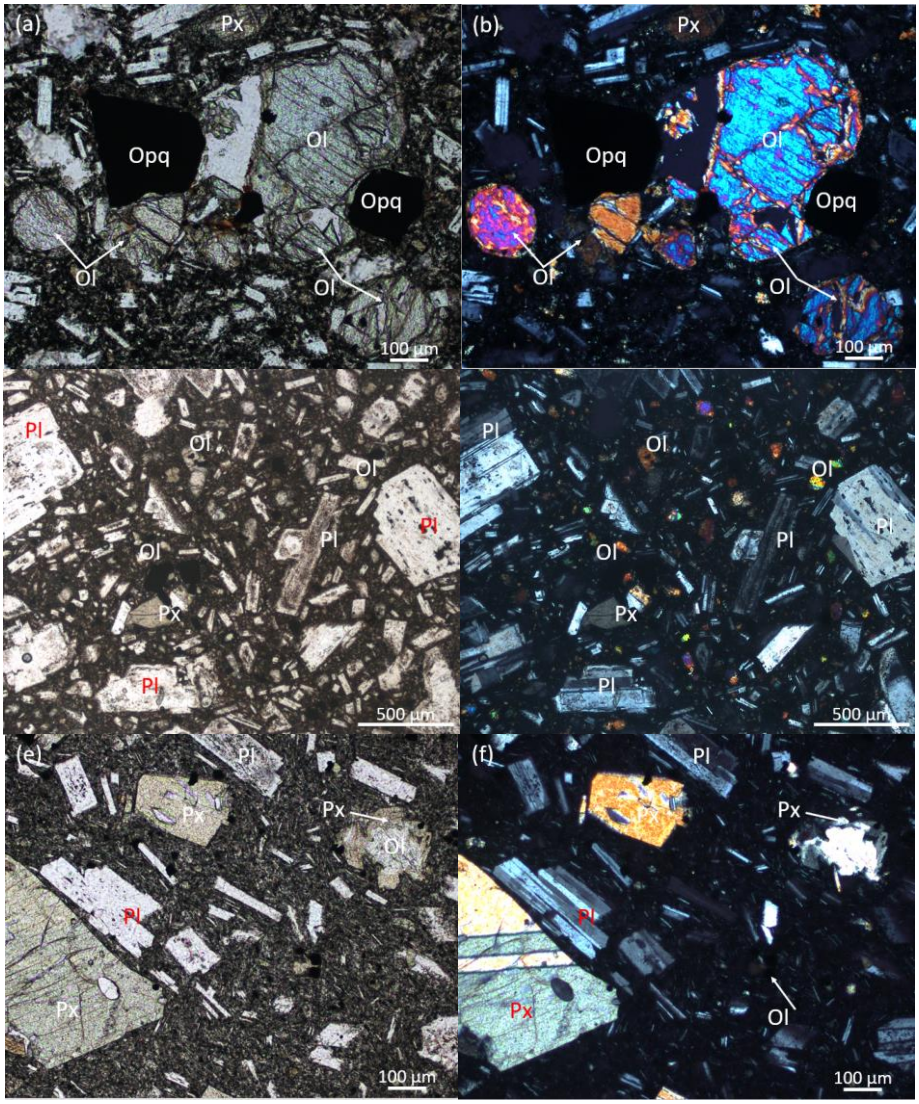

Figure 4 **(a)** and **(b)** Photomicrographs of basalt (GA-TU 1). **(c)** and **(d)** Photomicrographs of basaltic andesite (MTG-3). **(e)** and **(f)** Photomicrographs of andesite (BEL-4). Ol, olivine; Pl, plagioclase; Px, pyroxene; Opq, opaque mineral.

Medium-K basaltic andesite (Figure 4). The samples of medium-K basaltic andesite consist of Al7, Pl, Al10 and Al11 lava units. The group ranges from 52.41-54.59 wt.% SiO_2 and identified as low/high-Sc type. All rocks of this group are aluminous rich. Phenocrysts of this group are composed of olivine (Fo59-79), plagioclase (An43-85), a small amount of augite (Mg#70-77) and enstatite (65-

76). Olivine is zoned, often with reaction rims of clinoenstatite and symplectitic intergrowth of Fe-Ti oxide or pigeonite. Plagioclase phenocrysts are normal zoning from core to rim-crystal but compositional inversion in mid-crystal. They frequently display coarse sieve texture and glomerocrysts in all samples and fine sieve texture, resorption surface and rounded zone corner in several samples. Compared with the pyroxenes of high-Al basalts, the pyroxenes from basaltic andesitic are less Al-rich and slightly less Ti-rich. Moreover, they show a slightly increasing in Mg content in the mid-crystal.

Andesite (Figure 4). Al4, Al9 and Al14 lava units have andesitic composition with 57.61-60.09 wt.% SiO_2. The andesites are phenocryst-rich (28-43% volume) and dominated by plagioclase. The plagioclase phenocrysts (An30-86) are highly sieved (dominantly by fine sieve texture), oscillatory zoning and compositional inversion of Ca within mid-crystal. Rarely olivine is present (<2% volume) with reaction rims of clinoenstatite and pigeonite. Augite, enstatite and titanomagnetite phenocrysts are found in all the samples. Only in Al14 samples (lava of 1963 eruption), amphibole and xenolith are present. In general, the amphibole phenocrysts are hornblendes. They occur as micro-phenocrysts and appear to be the product of late-stage crystallization in H_2O-saturated condition. They have reaction rims composed of augite, feldspar and symplectitic intergrowth of titanomagnetite. Moreover, olivine xenocrysts with the highest forsterite content (Fo95) are found in the andesite xenolith in Al14 samples. These olivine xenocrysts are more magnesian than the other olivine phenocrysts. The high forsterite content of olivine may have crystallized from ultramafic rocks of presumed mantle origin [9].

Based on its stratigraphic position [3] the samples likely correspond to Al4, Al7, Pl, Al9, Al10, Al11, Al12, and Al14 lava units (Table 1). Lavas of Agung changed in composition throughout the eruption from andesite to basaltic-andesite and basalt i.e. the basaltic magma of the AD 1843 eruption differentiated into andesitic composition of the AD 1963 eruption. This open system behavior of Agung volcano includes magmatic recharge (mixing) recorded in minerals composition and micro-textures.

Crystal zoning reflects compositional changes in the mineral from core to rim-crystal [10]. Plagioclase, olivine, and pyroxene phenocryst of Agung's lava record normal zoning from core to rim-crystal but there are compositional inversions within mid-crystals. This condition suggests a more calcic magma injection, often considered to be synonymous with the recharge of more mafic magma, during the solidification process. It can be interpreted as open system process.

Plagioclase phenocrysts display a wide range of textures for investigating magma dynamics (Figure 5). Dissolution surfaces are found in most plagioclase phenocrysts and are described as coarse sieve and fine sieve textures. Coarse sieve interprets as a result of dissolution by the varying rate of adiabatic decompression during magma ascending into the shallower magma storage.

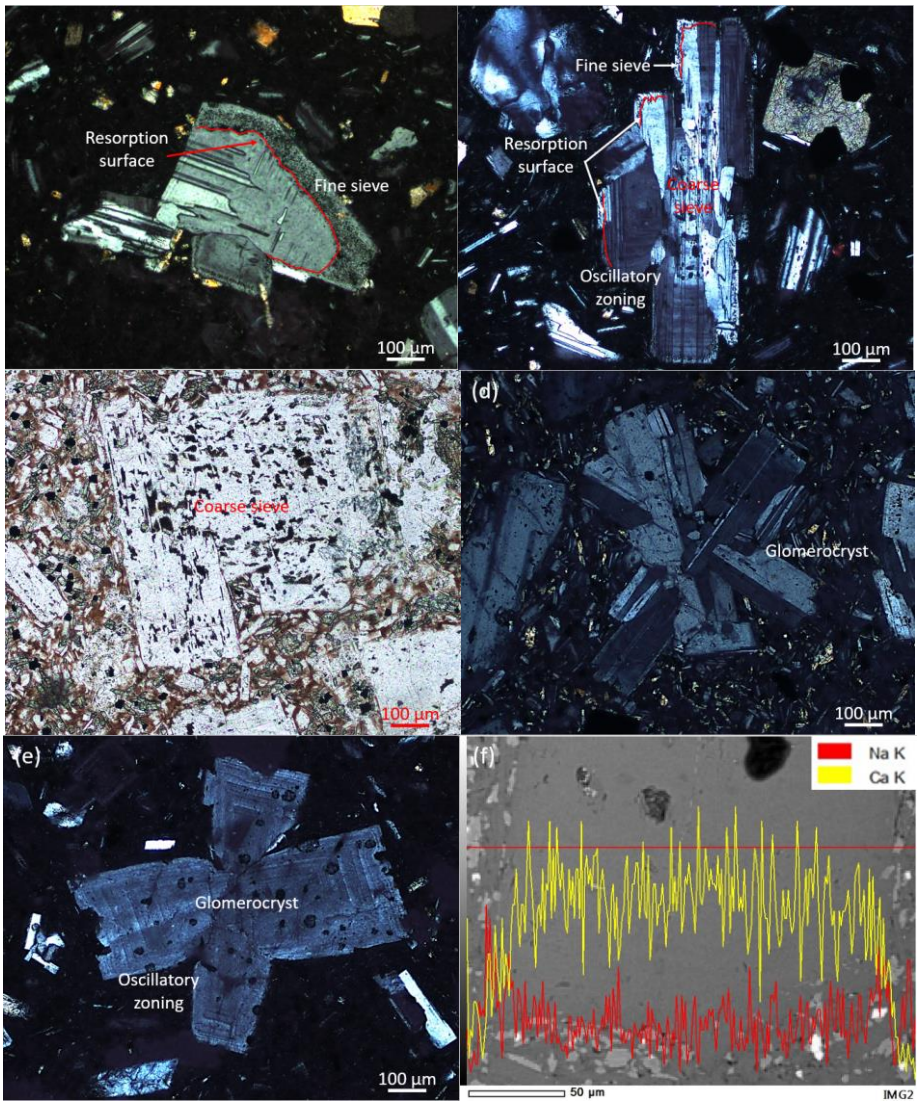

Figure 5 **(a)-(e)** Photomicrographs of various micro-textures in plagioclase phenocrysts. **(f)** Line analysis of plagioclase phenocryst show increases of Ca content in the mid mineral.

However, fine sieve interprets as a result of dissolution due to reaction with more calcic magma [11]. These sieve textures are frequently found at the core, mid or rim of plagioclase phenocrysts. The resorption surface is frequently found as the irregular surface at the outer edge of the fine sieve domain and the fine oscillatory zoning. Moreover, the fine oscillatory zoning is developed from the dynamic process such as crystallization from melt that was undergoing rhythmic changes in temperature or $P(H_2O)$ or composition and kinetic process such as local incremental diffusion-controlled kinetic growth at the crystal-melt interface in response to near equilibrium condition [11]. The presence of fine sieve texture and resorption surface are evidence for the recharge of more mafic magma into the shallower magma storage.

Olivine crystals can respond to diffusional re-equilibration, forming reaction rims or dissolution. These processes indicate open system behaviour [10]. Many olivine phenocrysts of Agung's lava have reaction rims of clinoenstatite or pigeonite, some texture less (Figure 6 and 7). Olivine phenocrysts in the basaltic andesitic lava also show symplectitic intergrowth of titanomagnetite within reaction rims of clinoenstatite or pigeonite (Figure 7). It serves as evidence for disequilibrium and indicates a different state of oxygen fugacity during crystallization from core to rim [12].

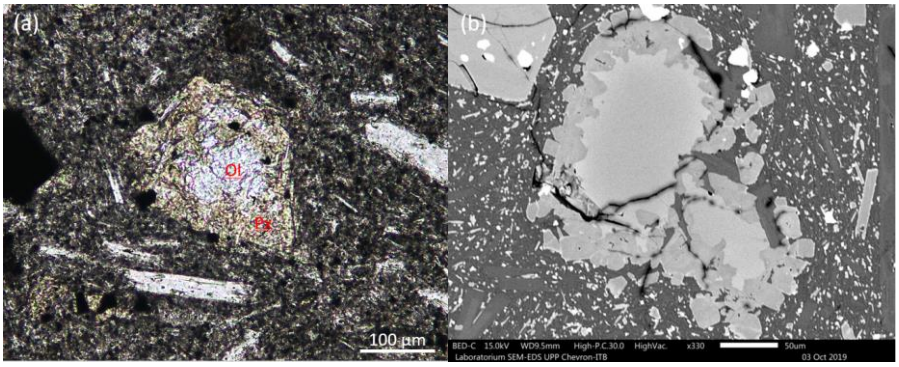

Figure 6 Reaction rims of olivine phenocrysts. **(a)** Photomicrograph of olivine phenocryst with thick reaction rim of pyroxene. **(b)** BED image of olivine phenocryst with thick reaction rim of clinoenstatite.

Orthopyroxene rim of olivine phenocrysts in basaltic andesitic or andesitic lava suggests mixing between basaltic and more silicic magma. Moreover, many olivine phenocrysts show a slightly increasing in Mg content in the mid-crystal that indicate recharge of more mafic magma during crystal growth. The presence of olivine crystals in intermediate to silicic magma is often taken as evidence for influx of more mafic magma [10].

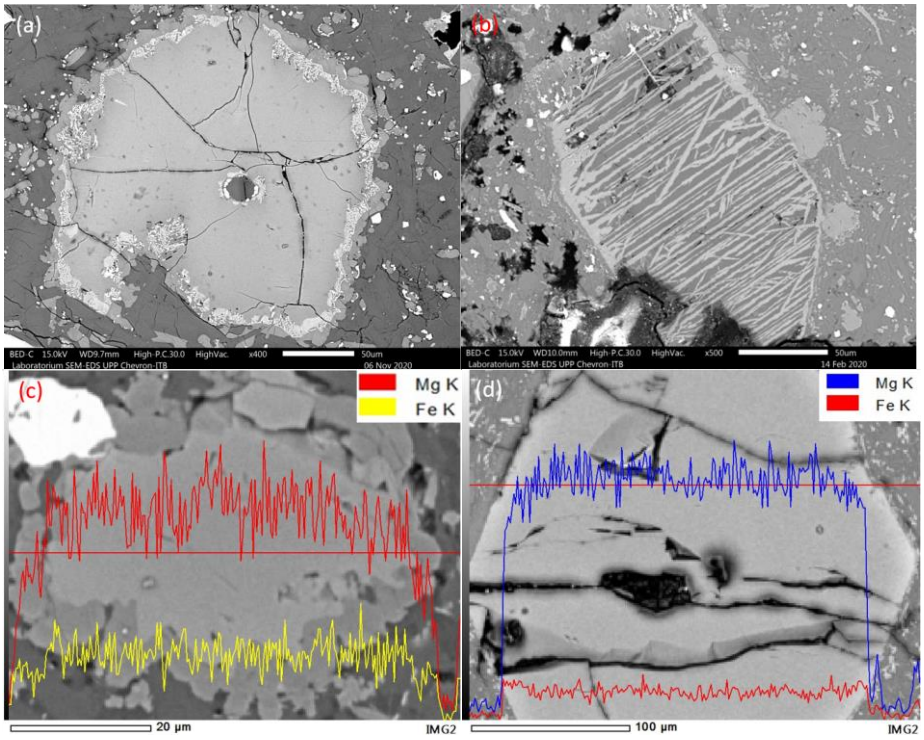

Figure 7 **(a)** BED image of of olivine phenocryst with reaction rim of clinoenstatite.and symplectitic intergrowth of titanomagnetite. **(b)** BED image of xenocryst olivine (Fo95) with lamella of lower forsterite content in the AD 1963 andesitic lava. **(c)** and **(d)** Line analyses of olivine phenocryst show slightly increasing in Mg content in the mid mineral.

Volatile-bearing minerals such as hornblende are particularly useful tools to constrain the syn-eruptive magma ascent rate because they become unstable as the concentration of dissolved water in the melt decreases during decompression. If magma ascends at a sufficiently slow rate, reaction rims of pyroxene, plagioclase and Fe-Ti oxides may develop around a hornblende crystal where it is in contact with melt [13] [14]. Hornblende with thinner reaction rims was interpreted to have originated from the main pulse of ascending magma, whereas the population of hornblende characterized by thicker rims was interpreted to have originated from batches of leftover or stalled magma in conduit [14].

Hornblende phenocrysts are only present in andesitic lava of the AD 1963 eruption. There are two types of hornblende phenocrysts, i.e. with thick opacitic rim and thick reaction rim of augite, plagioclase and symplectitic intergrowth of

titanomagnetite (Figure 8). First, the opacitic rim is described by the appearance of fine-grained magnetite [13]. This condition suggests a prolonged disequilibrium state when the magma ascended into storage depth outside amphibole stability. Second, thick reaction rims of augite, plagioclase and symplectitic intergrowth of titanomagnetite interpret to result from a heating event of leftover magma. Reaction rims are composed of orthopyroxene and plagioclase, with lesser amounts of Fe-Ti oxides produced during decompression [15].

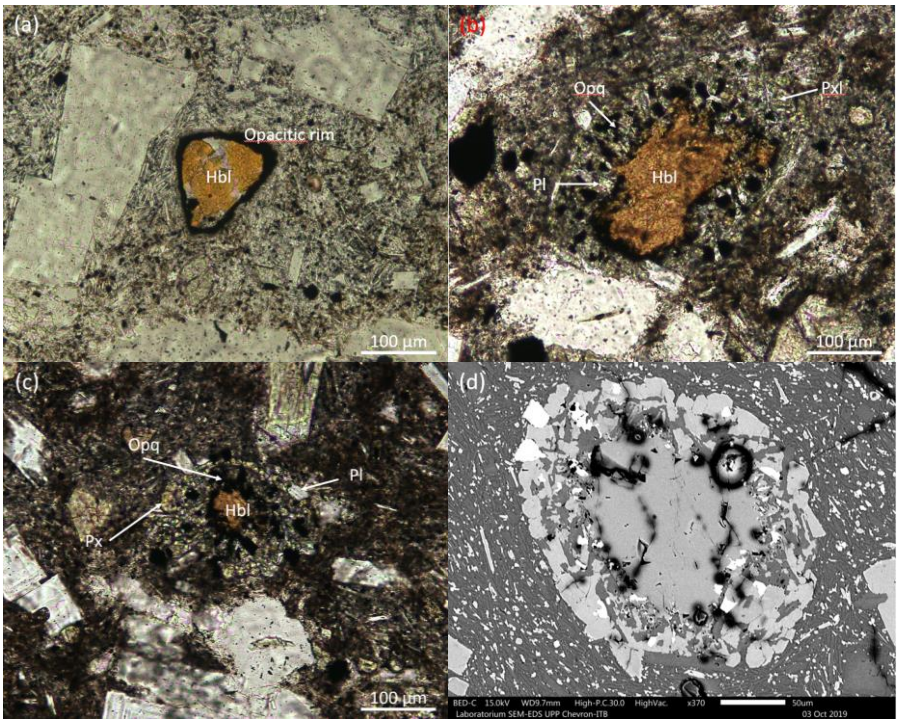

Figure 8 **(a)** Opacitic rim in hornblede. **(b)-(d)** Photomicrographs and BED image of thick reaction rim that composed of augite, plagioclase and titanomagnetite.

5 Conclusion

Agung volcano has three group of magma composition, i.e., andesite, basaltic-andesite and basalt. During the eruption before AD 1040 and AD 1963 there were changing magmatic composition from andesite to basaltic andesite, then basalt and andesite. The combined results between petrological and geochemical analyses show strong evidence for open system characteristics and disequilibrium condition between mineral and injected magma or leftover melt.

Plagioclase phenocrysts record wide range of textures and composition. There are many various micro-textures in plagioclase that can be described. Many plagioclase and olivine phenocrysts in all three groups are zoned from core to rim with compositional inversion in mid. Plagioclase phenocrysts dominantly display sieve texture and resorption surface due to dissolution and fine oscillatory zoning or glomerocrysts due to convective flow in the shallower magma chamber. Olivine phenocrysts display three types of reaction rims. i.e. pigeonite reaction rims, clinoenstatite with or without symplectitic intergrowth of titanomagnetite and texture less crystal. These textures may support the open system behavior and disequilibrium between olivine and the leftover magma in the magma chamber. Hornblende phenocrysts are only found in the AD 1963 andesitic lava. It strongly indicated that the AD 1963 andesitic magma was differentiated from leftover more mafic magma. Other evidence that supports this interpretation is thick reaction rims of augite, plagioclase and titanomagnetite in hornblende due to the heating event of leftover magma. However, thick opacitic rims suggest mineral-melt disequilibrium during magma ascending.

References

[1] Fontijn, K., Costa, F., Sutawidjaja, I., Newhall, C. G., & Herrin, J. S., *A 5000-year record of multiple highly explosive mafic eruptions from Gunung Agung (Bali, Indonesia): implication for eruption frequency and volcanic hazard*, Bulletin of Volcanology, **77**(59), Jun. 2015.

[2] Geiger, H., Troll, V. R., Jolis, E. M., Deegan, F. M., Harris, C., Hilton, D. R. & Freda, C., *Multi-level magma plumbing at Agung and Batur volcanoes increases risk of hazardous eruptions*, Scientific Report, **8**, pp. 1-14, Jul. 2018.

[3] Nasution, A., Haerani, N., Mulyadi, D., & Hendrasto, M., *Geological map of Agung volcano, Bali*, Directorate of Volcanology and Geological Hazard Mitigation, Bandung, 2004.

[4] Syracuse, E. M. & Goeffrey, A. A., *Global compilation of variations in slab depth beneath arc volcanoes and implications*, Geochemistry, Geophysics, Geosystems, **7**(5), pp. 1-18, May 2006.

[5] Verma, S. P. & Verma S. K., *First 15 probability-based multidimensional tectonic discrimination diagrams for intermediate magmas and their robustness against post emplacement compositional changes and petrogenetic processe*s, Turkish Journal of Earth Sciences, **22**, pp. 931-995, Oct 2013.

[6] Foden, J. D., *The Petrology of The Calcalkaline Lavas of Rindjani Volcano, East Sunda Arc: A model for Island Arc Petrogenesis*, Journal of Petrology, **24**(1), pp. 98-130, 1983.

[7] Le Bas, M. J., Le Maitre, R. W. & Streckeisen, A., *A chemical classification of volcanic rocks based on the Total Alkali-Silica diagram*, Journal of Petrology, **27**, pp. 745-750, 1984.

[8] Peccerillo, A. & Taylor, S. R., *Geochemistry of Eocene calc-alkaline volcanic rocks from the Kastamonu area, northern Turkey*. Contributions to Mineralogy and Petrology, **58**, 63-81, 1976.

[9] Deer, W. A., Howie, R. A. & Zussman, J. *An introduction to the rock forming mineral*, ed.3, Mineralogical Society of Great Britain and Ireland, 2013.

[10] Streck, M. J., *Mineral textures and zoning as evidence for open system processes*, Minerals, inclusions and volcanic processes, Putirka, K. D. & Tepley III, F. J., eds., Walter de Gruyter GmbH & Co KG, pp. 595-622, 2018.

[11] Renjith, M.L., *Micro-texture in plagioclase from 1994-1995 eruption, barren island volcano: evidence of dynamic magma plumbing system in the Andaman subduction zone*, Geoscience Frontier, **5**, pp. 113-126, 2014.

[12] Perugini, D. Busa, T., Poli, G. & Nazzareni S., *The role of chaotic dynamics and flow fields in the development of disequilibrium textures in volcanic rocks*, Journal of Petrology, **44**(4), p. 733-756, Apr. 2003.

[13] Rutherford, M. J. & Devine, J. D., *The role of chaotic dynamics and flow fields in the development of disequilibrium textures in volcanic rocks*, Journal of Petrology, **44**(8), pp. 1433-1454, 2003.

[14] Szramek, L. & Browne, B., *Rates of magma ascent and storage*, The Encyclopedia of Volcanoes (Second Edition), Sigurdsson, H., ed., Academic Press, pp. 2013-214, 2015.

[15] Browne, B., Gardner, J. E. & Larsen, J. F. *Amphibole reaction rims in response to decompression compared to heating: an experimental approach*, AGU Fall meeting, 2003.